EPAS-FINITE ELEMENT PROGRAM FOR ANALYSIS OF NONLINEAR BEHAVIOR OF NUCLEAR POWER PIPING

G. YAGAWA, Y. ANDO

Department of Nuclear Engineering, University of Tokyo, Hongo, Bunkyo-ku, Tokyo, Japan

T. WATANABE, S. ISHIWATA

Century Research Corporation, Nihonbashi-honcho, Tokyo, Japan

SUMMARY

As well known, the finite element methods are costly especially in inelastic structural analyses. Moreover, it is often necessary to calculate the local phenomena of stress and strain in the whole structure, e.g. the crack analysis in the pressure vessels and piping. In such kinds of analyses, the three-dimensional elements are necessarily utilized near the local part of the structure. In this context, several researchers have developed the economical finite element methods based upon the so-called tying technique which is to connect the different types of elements, e.g. the solid elements with the shell elements, the shell elements with the beam elements, etc. In this technique, it is necessary to prepare the special input data in order to bring into relation the different kinds of elements, which often require cumbersome work in such complex structures as pressure vessels and piping.

The purpose of this paper is to discuss the alternative technique to connect the different kinds of elements using the fictitious elements without occupied volume, so that one can considerably reduce the number of unknowns in the simultaneous equation regarding the finite element method without any troublesome preparation of input data. In other words, superior elements typified by the isoparametric solid elements are arranged only at such an important regions as near crack parts in the whole structure, while the other part of the structure is discretized with the use of one- or two-dimensional lower class of elements, e.g. the beam, plate and shell elements. The connection of the different types of elements is pursued with the help of the fictitious elements placed between the real elements, the characteristics of which are determined by employing the Lagrange multiplier concept. Unknowns of the resulting simultaneous equation consist of usual nodal displacemtns of the whole structure together with the generalized coordinates regarding the Lagrange multipliers for the fictitious elements.

Three kinds of fictitious elements are developed in this paper. These are for connections between the flat shell elements and the solid elements, the beam elements and the flat shell elements, and the beam elements and the solid elements, respectively. These fictious elements are incorporated into the finite element program EPAS (Elastic Plastic Analysis System).

In order to verify and qualify the EPAS, the elastic plastic analyses are made for the pipes with circumferential cracks under mechanical or thermal load. Theoretical results agree favourably with the measured values. Comparison of central processor time for the elastic-plastic calculation shows that one can reduce the computer cost less than one third with the present method.

1. INTRODUCTION

The analyses of the local stress and strain concentrations in the complex piping of reactor plants have been emphasized recently, since the intergranular stress corrosion cracks were discovered in the inside surface of the piping made of the austenitic stainless steels. The finite element method is known to be powerful for this kind of 3-dimensional as well as nonlinear stress and strain analyses except for the computer cost. In this regard, Hibbitt, et al.[(1)(2)] have developed a technique to combine the different types of elements, where they use the constraint equations generated by enforcing compatibility directly in the governing stiffness equation, removing one degree of freedom from that equation for each constraint condition. Chen and Schnobrich[(3)] have utilized a special layered system in the region of the intersection in the cylinders, while 2-dimensional shell elements are used throughout the remainder of the structure.

In this paper, an alternative technique is proposed to combine the different kinds of elements using the fictitious connection elements without occupied volume, the characteristics of which are determined by the aid of the Lagrange multipliers. Three kinds of the connection elements are developed and incorporated into the program EPAS (Elastic Plastic Analysis System).

In order to verify and qualify the EPAS, the elastic plastic analyses are made for the pipes with circumferential cracks under mechanical or thermal load. The computed results agree favourably with the measured values. Comparison of central processor time for the elastic-plastic calculation shows that one can reduce the computer cost less than one third using the EPAS.

[NOMENCLATURE]

[B]:transformation matrix between strain and displacement. E^{e}_{ijkl}:elastic coefficient. f:yield function. g:plastic potential. [I]:unit matrix (6×6). $|J|$:Jacobian determinant. $\hat{J}_{mn}$:inversed matrix of Jacobian matrix. n_j:outerward normal unit vector on surface S. $\bar{P}_i$:body force. {q}:nodal displacement. {r}:generalized coordinates of fictious element. S_u:displacement boundary. S_σ:mechanical boundary. $S^{(12)}$:fictitious boundary surface. T:temperature. T_i:traction. u_i:displacement. V:region of continuum. $(\ )^e$:elastic component. $(\ )^{ep}$:elastic-plastic component. $(\ )^p$:plastic component. $(\ )^T$:thermal component. $(\ )^t$:transposed matrix. $(\bar{\ })$:prescribed value. $(\ )_{,i}$:partial differentiation with respect to coordinates i. $\Delta(\ )$:incremental value. $\delta(\ )$:virtual quantity. $(\ )^{(\alpha)}$:quantity belonging to fictious region α. σ_{ij}:stress. ε_{ij}:strain. λ_i:Lagrange multiplier. $\{\lambda\}$:column matrix of Lagrange multiplier. θ_i:rotation. $[\phi]$, $[\psi]$ and $[\Omega]$:interpolation matrix.

2. THEORETICAL BACKGROUND

2.1 Basic Equations and Variational Principle

The equilibrium equation and the strain-displacement relation for the three-deminstional continuum are given in incremental form as follows

$$\Delta\sigma_{ij,j} + \Delta\bar{P}_i = 0, \quad \Delta\varepsilon_{ij} = \frac{1}{2}(\Delta u_{i,j} + \Delta u_{j,i}) \qquad \text{in V} \qquad (1),\ (2)$$

where the small displacement assumption is made for simplicity. The strain increment is assumed to be decomposed into three components as follows

$$\Delta\varepsilon_{ij} = \Delta\varepsilon^{e}_{ij} + \Delta\varepsilon^{p}_{ij} + \Delta\varepsilon^{T}_{ij} = \Delta\varepsilon^{ep}_{ij} + \Delta\varepsilon^{T}_{ij} \qquad \text{in V} \qquad (3)$$

The stress increment is written as

$$\Delta\sigma_{ij} = E^{ep}_{ijkl}\, \Delta\varepsilon^{ep}_{kl} + G^{ep}_{ij}\, \Delta T \qquad \text{in V} \qquad (4)$$

where E^{ep}_{ijkl} and G^{ep}_{ij} are appropriate tensors obtained with the help of the von Mises yield criterion and the associated flow rule.

According to the Cauchy's formula, the traction force increment is related with the stress increment on an arbitrary sections in V as follows

$$\Delta T_i = \Delta\sigma_{ij}\, n_j \qquad \text{on S} \qquad (5)$$

The geometrical and the mechanical boundary conditions can be written, respectively, as follows

$$\Delta u_i = \Delta\bar{u}_i \qquad \text{on } S_u, \qquad \Delta T_i = \Delta\bar{T}_i \qquad \text{on } S_\sigma \qquad (6), (7)$$

The principle of virtual work in this case is given as

$$\int_V \Delta\sigma_{ij}\, \delta(\Delta\varepsilon_{ij})dv - \int_V \Delta\bar{P}_i \delta(\Delta u_i)dv - \int_{S_\sigma} \Delta\bar{T}_i\, \delta(\Delta u_i)dS = 0 \qquad (8)$$

Provided that the continuum is fictitiously devided into two parts as shown in Fig. 1, the following principle of virtual work holds.

$$\sum_{\alpha=1}^{2} [\int_{V^{(\alpha)}} \Delta\sigma^{(\alpha)}_{ij} \delta(\Delta\varepsilon^{(\alpha)}_{ij})dV - \int_{V^{(\alpha)}} \Delta\bar{P}^{(\alpha)} \delta(\Delta u^{(\alpha)}_i)dV -$$

$$\int_{S_\sigma^{(\alpha)}} \Delta\bar{T}^{(\alpha)}_i \delta(\Delta u^{(\alpha)}_i)dS] - \delta\int_{S^{(12)}} \Delta\lambda_i (\Delta u^{(1)}_i - \Delta u^{(2)}_i)dS = 0 \qquad (9)$$

where the continuity conditions between the regions, α=1 and 2, are taken into account in Eq. (9).

Application of Eq. (9) to the finite element formulation is described in what follows.

2.2 Finite Element Equation

In order to combine different types of elements in a single structure, we show here the finite element formulation based on Eq. (9).

The incremental displacements of the regions $V^{(\alpha)}$, α=1 and 2, and the fictitious surface $S^{(12)}$ between $V^{(1)}$ and $V^{(2)}$ are, respectively, discretized as follows

$$\{\Delta u^{(\alpha)}\} = [\phi^{(\alpha)}]\{\Delta q^{(\alpha)}\} \qquad \text{in } V^{(\alpha)},\ \alpha = 1 \text{ and } 2 \qquad (10)$$

$$\{\Delta u^{(\alpha)}\} = [\psi^{(\alpha)}]\{\Delta q^{(\alpha)}\} \qquad \text{on } S^{(12)},\ \alpha = 1 \text{ and } 2 \qquad (11)$$

Similarly, the Lagrange multipliers on $S^{(12)}$ can be interpolated as follows[4]

$$\{\Delta\lambda\} = [\Omega]\{\Delta\gamma\} \qquad \text{on } S^{(12)} \qquad (12)$$

The strain-displacement and the stress-strain relations are, respectively, written by the use of Eqs. (2), (4) and (10) as follows

$$\{\Delta\varepsilon^{(\alpha)}\} = [B^{(\alpha)}]\{\Delta q^{(\alpha)}\} \qquad \text{in } V^{(\alpha)},\ \alpha = 1 \text{ and } 2 \qquad (13)$$

$$\{\Delta\sigma^{(\alpha)}\} = [E^{ep(\alpha)}]([B^{(\alpha)}]\{\Delta q^{(\alpha)}\} - \{\Delta\varepsilon^{T(\alpha)}\}) + \{G^{(\alpha)}\}\Delta T^{(\alpha)}$$
$$\text{in } V^{(\alpha)},\ \alpha = 1 \text{ and } 2 \qquad (14)$$

where $[B^{(\alpha)}]$ is the transformation matrix between the nodal displacement and the strain of the region $V^{(\alpha)}$.

Substituting Eqs. (10)∼(14) into Eq. (9), we obtain the following equation.

$$\sum_{\alpha=1}^{2} \delta\{\Delta q^{(\alpha)}\}^t([K^{(\alpha)}]\{\Delta q^{(\alpha)}\} + [\hat{K}^{(\alpha)}]\{\Delta\gamma\} + \{\Delta F^{(\alpha)}\}) +$$
$$\delta\{\Delta\gamma\}^t \sum_{\alpha=1}^{2} [\hat{K}^{(\alpha)}]^t\{\Delta q^{(\alpha)}\} = 0 \tag{15}$$

where

$$[K^{(\alpha)}] = \int_{V^{(\alpha)}} [B^{(\alpha)}]^t[E^{ep(\alpha)}][B^{(\alpha)}]dV \qquad ,\alpha = 1 \text{ and } 2 \tag{16}$$

$$[\hat{K}^{(1)}] = -\int_{S^{(12)}} [\psi^{(1)}]^t[\Omega]dS, \qquad [\hat{K}^{(2)}] = \int_{S^{(12)}} [\psi^{(2)}]^t[\Omega]dS \qquad (17), (18)$$

$$\{\Delta F^{(\alpha)}\} = -\int_{V^{(\alpha)}} [B^{(\alpha)}]^t[E^{ep(\alpha)}]\{\Delta\varepsilon^{T(\alpha)}\}dV + \int_{V^{(\alpha)}} [B^{(\alpha)}]^t\{G^{(\alpha)}\}\Delta T^{(\alpha)}dV -$$
$$\int_{V^{(\alpha)}} [\phi^{(\alpha)}]^t\{\Delta\bar{P}^{(\alpha)}\}dV - \int_{S_\sigma^{(\alpha)}} [\phi^{(\alpha)}]^t\{\Delta\bar{T}^{(\alpha)}\}dS \quad , \alpha = 1 \text{ and } 2 \tag{19}$$

Since $\delta\{\Delta q^{(\alpha)}\}$ and $\delta\{\Delta r\}$ are arbitrary, Eq. (15) can be written as follows

$$\begin{bmatrix} [K^{(1)}] & [\ 0\ ] & [\hat{K}^{(1)}] \\ & [K^{(2)}] & [\hat{K}^{(2)}] \\ \text{Sym.} & & [\ 0\ ] \end{bmatrix} \begin{Bmatrix} \{\Delta q^{(1)}\} \\ \{\Delta q^{(2)}\} \\ \{\ \Delta\gamma\ \} \end{Bmatrix} = \begin{Bmatrix} \{\Delta F^{(1)}\} \\ \{\Delta F^{(2)}\} \\ \{\ 0\ \} \end{Bmatrix} \tag{20}$$

2.3 Fictitious Elements for Connections

The fictitious connection elements which have no volume have been developed for the purpose of the connections between the flat shell and the solid elements, between the flat shell and the beam elements and between the beam and the solid elements. As an example of these special elements, we describe here the connection element between the flat shell and the beam elements. This element, which is conceptually a triangular prism as shown in Fig. 2, connects the flat shell element to the 20-node solid element. The degree of freedom in the connection element is forty-two, i. e. three at each node on $S^{(12)}$ corresponding to the solid element, six at each node on $S^{(12)}$ corresponding to the flat shell element and six at the inside of the element. Provided that the flat shell and the solid elements correspond, respectively, to α=1 and 2, and $S_e^{(12)}$ represents the area occupied by one of the connection elements, $\{\Delta u^{(\alpha)}\}$ and $\{\Delta q^{(\alpha)}\}$, α=1 and 2, in Eq. (11) can be written as follows

$$\{\Delta u^{(1)}\} = \{\Delta u^{(2)}\} = \Delta\lfloor u_1, u_2, u_3, \theta_1, \theta_2, \theta_3\rfloor^t \qquad \text{on } S_e^{(12)} \tag{21}$$

$$\{\Delta q^{(1)}\} = \Delta\lfloor u_1^9, u_2^9, \ldots\ldots, \theta_3^9, u_1^{10}, u_2^{10}, \ldots\ldots, \theta_3^{10}\rfloor^t \qquad \text{on } S_e^{(12)} \tag{22}$$

$$\{\Delta q^{(2)}\} = \Delta\lfloor u_1^1, u_2^1, u_3^1, \ldots\ldots, u_1^8, u_2^8, u_3^8\rfloor^t \qquad \text{on } S_e^{(12)} \tag{23}$$

$$S^{(12)} = \sum_{e=1}^{n} S_e^{(12)} (n = \text{total number of connection elements on } S^{(12)}) \tag{24}$$

where the superscripts and the subscripts on u and θ denote the nodal numbers and the coordinates, respectively (see Fig. 2). The interpolation function $[\psi^{(\alpha)}]$, α=1 and 2, can be written as follows

$$[\psi^{(1)}] = [\overset{*}{\psi}_1[I], \overset{*}{\psi}_2[I]], \quad [\psi^{(2)}] = [[\psi_1], [\psi_2], \ldots\ldots, [\psi_8]] \quad \text{on } S_e^{(12)} \tag{25), (26}$$

where

$$\overset{*}{\psi}_1 = (1 - \frac{\hat{x}}{\ell}), \ \overset{*}{\psi}_2 = \frac{\hat{x}}{\ell}, \ \ell = |\hat{x}^{10} - \hat{x}^9| \tag{27}$$

$$[\psi_i] = \begin{bmatrix} \hat{\psi}_i & 0 & 0 & 0 & 0 & -\frac{a_i}{2} \\ 0 & \hat{\psi}_i & 0 & 0 & 0 & \frac{b_i}{2} \\ 0 & 0 & \hat{\psi}_i & a_i & -b_i & 0 \end{bmatrix}^t, \ i = 1,2, \ldots\ldots, 8 \tag{28}$$

$$a_i = \hat{J}_{21}\frac{\partial\hat{\psi}_i}{\partial\xi} + \hat{J}_{22}\frac{\partial\hat{\psi}_i}{\partial\eta}, \ b_i = \hat{J}_{11}\frac{\partial\hat{\psi}_i}{\partial\xi} + \hat{J}_{12}\frac{\partial\hat{\psi}_i}{\partial\eta} \tag{29}$$

Here, $\hat{x}$ is the local coordinate as shown in Fig. 2 and $\hat{\psi}_i$ is the shape function of the Serendipity two-dimensional 8-node (quadratic) element[5], the local coordinates of which are shown in Fig. 3.

If the Lagrange multipliers are assumed to be constant in the connection elements, $[\Delta\lambda]$, $[\Delta\gamma]$ and $[\Omega]$ in Eq. (12) are given, respectively, as follows

$$\{\Delta\lambda\} = \Delta\lfloor\lambda_1, \lambda_2, \ldots\ldots, \lambda_6\rfloor^t, \ \{\Delta\gamma\} = \Delta\lfloor\gamma_1, \gamma_2, \ldots\ldots, \gamma_6\rfloor^t, \ [\Omega] = [\ I\ ] \tag{30),(31),(32}$$

Substituting Eqs. (25) and (32) into Eq. (17) and Eqs. (26) and (32) into Eq. (18), respectively, we have

$$[\hat{K}^{(1)}] = -\sum_{e=1}^{n}\int_{S_e^{(12)}}[\psi^{(1)}]^t dS \quad \text{on } S^{(12)} \tag{33}$$

$$[\hat{K}^{(2)}] = \sum_{e=1}^{n}\int_{S_e^{(12)}}[\psi^{(2)}]^t dS = \sum_{e=1}^{n}\int_{-1}^{1}\int_{-1}^{1}[\psi^{(2)}]^t|J|d\xi d\eta \quad \text{on } S^{(12)} \tag{34}$$

where Eq. (24) is used.

3. NUMERICAL RESULTS

The numerical results using the finite element program EPAS are shown in this section. The elastic-plastic calculation is made on the basis of the isotropic material hardening and the mixed technique of the incremental and the initial stress methods.

3.1 Straight Pipe with a Through Crack Subjected to Internal Pressure and Shear Force

Using the two kinds of the connection elements, the elastic-plastic analysis is made on the cantilever pipe with a circumferential through wall crack as shown in Fig. 4. The material is 304 stainless steel, the uniaxial stress-strain relation of which is assumed as shown in Fig. 5. The pipe is first subjected to the internal pressure 100 kg/mm^2, and then the shear force P is applied to the pipe through the loading arm as shown in Fig. 4. From the symmetry of the structure, one half of the pipe is discretized using the two kinds of meshes as follows.

(a) Solid model (see Fig. 6.)

(b) Solid-shell-beam model (see Fig. 7.)

The crack opening displacements (C. O. D.) and the axial strains are depicted versus load with the experimental results in Figs. 8 and 9, respectively.

3.2 Straight Pipe with Semi-Elliptical Surface Cracks Subjected to Induction Heating

Consider the straight pipe made of stainless steel 304 (outer diameter = 318.5mm, thickness = 19mm), which has four semi-elliptical cracks in the circumferential direction in the inner surface as shown in Fig. 10. The length and the depth of the semi-elliptical cracks are, respectively, 14.4mm and 2.4mm. The material is assumed to have the temperature dependent stress-strain relations(6). We consider the case that the pipe is heated for 180 seconds by the induction heating coil which surrounds the pipe as shown in Fig. 10, while the inside of the pipe is cooled by the flowing water of 30°C with the velocity of 2m/sec. This experiment was carried out to study the crack behaviors under the induction heating stress improvement of nuclear primary piping(7).

First, the temperature histories are calculated using the axisymmetric finite elements as shown in Fig. 11. The elastic-plastic crack analysis is then carried out using the finite element mesh as shown in Fig. 12, in which only 1/16 of the pipe is discretized taking advantage of the symmetry. As shown in the figure, the 20-node solid and the flat shell elements are employed, respectively, near the crack and in the remainder of the structure. The fictitious connection elements are used between the solid and the flat shell elements. Fig. 13 depicts the calculated distributions of the crack opening displacements δ at the end of the heating (maximum) and at the time cooled down (residual). The result using the axisymmetric elements is also plotted for comparison in the figure.

4. CONCLUSIONS

The merits of using the EPAS reported in this paper are summarized in what follows.

(1) Using the EPAS with the fictitious connection elements, one can reduce the computer cost less than one third without the loss of accuracy of the calculated results.

(2) The preparation of input data, which is often cumbersome in the 3-dimensional analyses of the complex structures with the conventional connection method between the different kinds of elements, e. g. the tying method, becomes much easier by using the connection elements adopted in the EPAS, since the connection elements in the EPAS can be used as if these are the usual elements.

[ACKNOWLEDGEMENT]

The authors wish to express their gratitude to the members of the 5SS, 6SS and 7SS Committees of the Japan Society of Welding Engineers for their valuable discussions. Special thanks are also due Mr. T. Umemoto, et al. of the IHI Co., Ltd. for their valuable experimental data and to Mr. H. Takeda of CRC for his fruitful comments on this study.

[REFERENCES]

(1) Hibbitt, H.D. and Marcal, P.V., AIAA 8th Aerospace Sciences Meeting, Paper No. 70-137 (1970).

(2) Hibbitt, H.D., et al., Proc. 2nd Int. Conf. on Pressure Vessel Technology, Part I, ASME, pp.239-251 (1973).

(3) Chen, H.C. and Schnobrich, W.C., Inelastic Behavior of Pressure Vessel and Piping Components, PVP-PB-028, ASME, pp.85-102 (1978).

(4) Yagawa, G. and Miyazaki, N., Int. J. Num. Meth. Engng., Vol.11, pp.1107-1115 (1977).

(5) Zienkiewicz, O.C., The Finite Element Method in Engineering Science, McGraw-Hill (1971).

(6) Report of Research Cooperation Subcommittee 46 on Research and Developement of Methods for Inelastic Structural Analysis, JSME (1977).

(7) Ando, Y., et al., 5th SMIRT, F2/5 (1979).

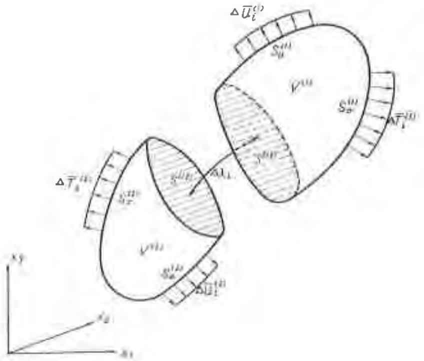

Fig. 1 Continum devided into two parts.

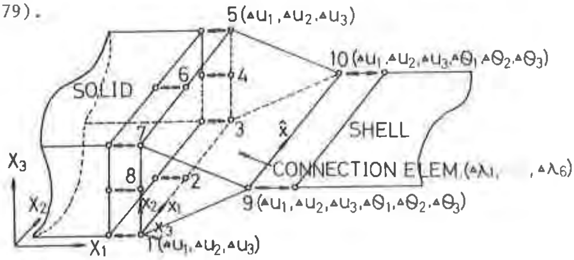

Fig. 2 Conception of connection element between solid and flat shell elements.

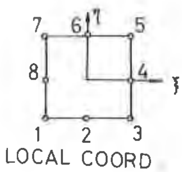

Fig. 3 Local coordinates.

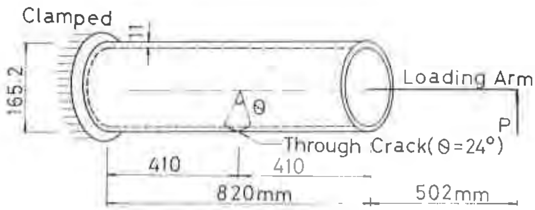

Fig. 4 Straight pipe with a through crack subjected to internal pressure and shear force.

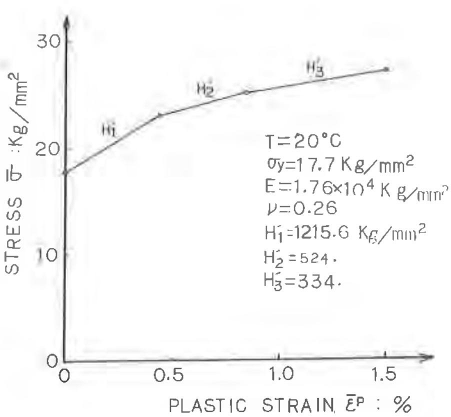

Fig. 5 Stress-plastic strain relation.

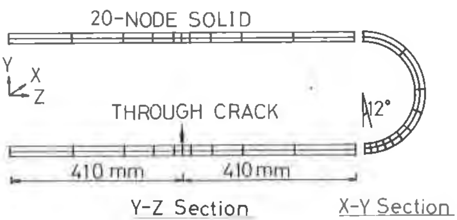

Fig. 6 Solid model.

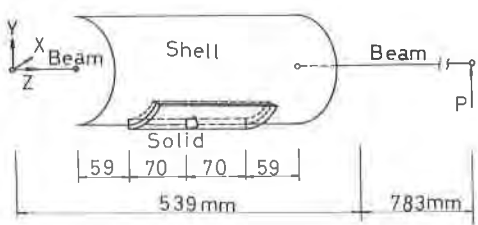

Fig. 7 Solid-shell-beam model.

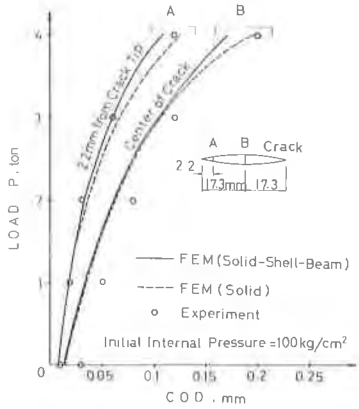

Fig. 8 Crack opening displacements vs. load.

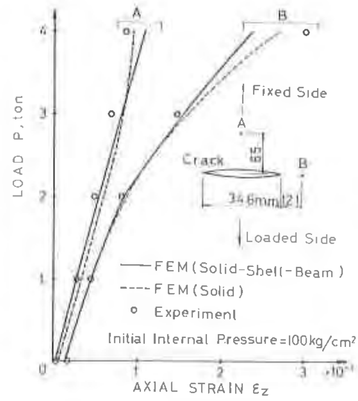

Fig. 9 Axial strains vs. load.

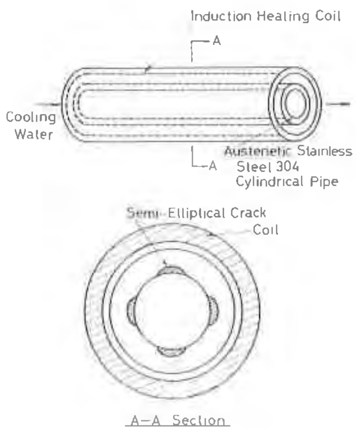

Fig.10. Straight pipe with semi-elliptical surface cracks subjected to induction heating.

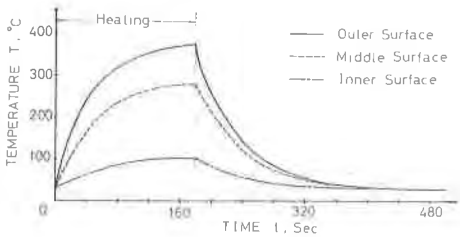

Fig.11 Temperature histories.

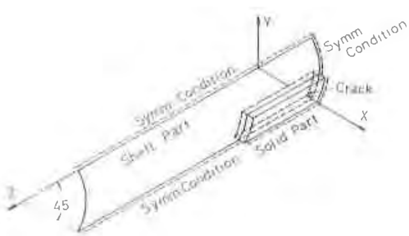

Fig.12 Solid-shell model.

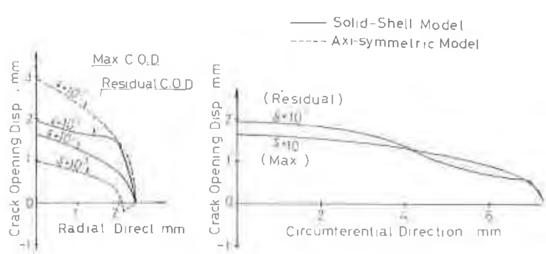

Fig.13 Distributions of crack opening displacements.